View metadata, citation and similar papers at core.ac.uk

brought to you by CORE

provided by Purdue E-Pubs

Purdue University
Purdue e-Pubs

International Compressor Engineering Conference | School of Mechanical Engineering

2008

Effect of Oil Feed Groove on Compressor Piston Lubrication

Bilgin Hacioglu
Arcelik Company

Zafer Dursunkaya
Middle East Technical University

Follow this and additional works at: https://docs.lib.purdue.edu/icec

Hacioglu, Bilgin and Dursunkaya, Zafer, "Effect of Oil Feed Groove on Compressor Piston Lubrication" (2008). *International Compressor Engineering Conference.* Paper 1887.
https://docs.lib.purdue.edu/icec/1887

This document has been made available through Purdue e-Pubs, a service of the Purdue University Libraries. Please contact epubs@purdue.edu for additional information.
Complete proceedings may be acquired in print and on CD-ROM directly from the Ray W. Herrick Laboratories at https://engineering.purdue.edu/Herrick/Events/orderlit.html

Effect of Oil Feed Groove on Compressor Piston Lubricaton

Bilgin Hacıoğlu[1*], Zafer Dursunkaya[2]

[1]Arçelik Company, Compressor Plant
Eskişehir, Turkey
Phone: 90 222 213 4664, Fax: 90 222 236 0344
E-mail: bilgin.hacioglu@arcelik.com

[2]Middle East Technical University, Mechanical Engineering Department
Ankara, Turkey
Phone: 90 312 210 5232, Fax: 90 312 210 1266
E-mail: refaz@metu.edu.tr

ABSTRACT

Oil feed grooves are implemented in reciprocating compressor piston applications to assure a constant supply of lubricating oil on bearing surfaces and decrease friction loss. In a hermetically sealed compressor, due to small clearances encountered, oil supply becomes critical in order to prevent the boundary lubrication. Due to the small size of the piston and small piston–cylinder clearance, a partial lubrication regime is present. In the current study, a model that solves Reynolds' equation for piston-cylinder sliding bearing for a compressor piston with oil feed groove is developed. A parametric study is carried out to investigate the effects of piston oil feed groove design parameters and then arrive at an improved piston performance by using alternative designs for the oil feed groove.

1. INTRODUCTION

The lateral motions of the piston during piston sliding motion inside a cylinder are named secondary dynamics. The simulation of piston secondary motion requires the solution of equations of motion of the piston in axial and lateral directions simultaneously. The sliding motion in axial direction is determined by analyzing the slider crank mechanism, and the equations of motion in lateral direction are solved coupled with the lubrication equation known as Reynolds' equation. In this study, Reynolds' equation is solved using a rigid piston-cylinder assumption. The equations of motion in lateral direction are solved using the calculated oil film hydrodynamic pressure, boundary contact pressure, cylinder gas pressure and inertia forces determined form slider crank dynamics and lubrication analyze.

In the field of lubrication phenomenon of a reciprocating piston there are many studies carried out in recent years especially for automotive applications. Goenka and Meernik (1992) [1] describe the analysis methods developed for piston lubrication analysis and compare the friction prediction of each of these methods with data obtained from an experimental rig designed to measure piston-assembly friction. Keribar and Dursunkaya (1992) [2] solve hydrodynamic lubrication problem and present a general model for the solution of secondary motion analysis of conventional and articulated piston assemblies. In the paper of Keribar and Dursunkaya (1992) [3] that is continuation of [2] a comprehensive model of piston is developed for use in conjunction with piston secondary dynamic analysis to characterize the effects of the skirt-cylinder oil film on piston motions. For the Reynolds' equation a finite difference solution is used and an asperity contact model is implemented to the solution to calculate the oil and contact pressure distribution in the skirt-bore oil film as a function of all input design parameters and positions and motions of the skirt relative to the cylinder. An integrated simulation methodology for the analysis of piston tribology is presented by Keribar, Dursunkaya and Ganapathy (1993) [4] that is comprised of coupled models of piston secondary dynamics, skirt oil film elasto-hydrodynamic lubrication and wristpin bearing hydrodynamics, developed earlier by the authors. The model predicts piston assembly secondary motions, piston skirt friction, skirt and wristpin oil film pressures, transient deformations, skirt-cylinder contact/impact pressures and skirt and cylinder wear loads. In the field of lubrication of compressor bearings, Duyar and Dursunkaya (2002), (2006) [5, 6] solve elasto-hydrodynamic lubrication problem for compressor small end bearing using finite difference solution of the Reynolds' equation for elastic pin problem. With a parametric, study they search the effects of design parameters of the connecting rod small end bearing.

2. MODELLING

The equation of the piston hydrodynamic lubrication problem is the Reynolds' equation for the oil film thickness and oil film pressure distributions. The following form of the Reynolds' equation is used, where θ is the piston circumferential coordinate, z is the piston axial coordinate. R is piston radius and U is piston sliding velocity in axial direction.

$$\frac{\partial}{\partial z}\left(h^3\frac{\partial P}{\partial z}\right)+\frac{1}{R^2}\frac{\partial}{\partial \theta}\left(h^3\frac{\partial P}{\partial \theta}\right)=-6\mu U\frac{\partial h}{\partial z}+12\mu\frac{\partial h}{\partial t} \quad (1)$$

Reynolds' equation is solved numerically to calculate film thickness and pressure distribution profiles around the piston. The second order derivatives are discreted using finite difference formulation for a selected mesh size of the lubricated regions of the thrust and anti-thrust planes on the piston. Only the side areas, corresponding to θ=100˚, of the piston is assumed to be lubricated. So the solution is carried only for these lubricated side areas for thrust and anti thrust sides both defined with *θ=100˚*.

The film thickness h includes the effect of connecting rod motions, bearing clearance and oil feed groove.

$$h(z,\theta,t)=h_{dyn}(z,\theta,t)+h_{grv}(z,\theta,t) \quad (2)$$

$$h_{dyn}(i,j)=c+(e+\Delta z.j\tan\lambda)\cos\theta \quad (3)$$

where c is radial clearance, e is eccentricity at piston center of mass, λ is piston tilt angle and θ is circumferential coordinate.

The piston is symmetric with respect to a symmetry plane dividing the thrust and anti thrust equally to *θ=50˚* areas. Hence, the boundary conditions for the solution of the lubrication equations are as following,

$$P=P_{sc};\ z=0 \quad (4)$$

$$P=P_{gas};\ z=L \quad (5)$$

$$P=\frac{(P_{gas}-P_{sc})}{L_h}z;\ \theta=50^\circ,\ 130^\circ \quad (6)$$

where, P_{sc} is the suction pressure inside the shell of the compressor, P_{gas} is the cylinder absolute gas pressure, L is the piston length, L_h is the length from piston head to groove. The linear distribution is considered only between the groove and piston head for the grooved piston at $\theta=50^\circ, 130^\circ$. Remaining pressures at these boundaries are taken as suction pressure.

In the cavitation region of the bearing, Half Sommerfeld assumption is used (Sommerfeld, 1904) [7],

$$P=0,\quad \text{if } P<0 \quad (7)$$

During operation, surfaces may come close to each other so that asperity contacts may occur or the surfaces may touch resulting in a boundary force created by the asperity contact pressures. In this case, boundary lubrication occurs and the load on the bearing is not only carried by the hydrodynamic force, but also by the boundary force that is quantified using a microcontact model. Microcontact models are useful for interpreting roughness characteristic of two interfacing rough surfaces in such terms as the mean real area of the contact, the contact density, the mean real pressure and the density of real contacts (McCool, 1988; Greenwood and Trip, 1971) [8, 9].

The model of Greenwood and Trip (1971) [9], is used for the calculation of boundary contact forces at the asperity contact regions of the finite difference mesh.

The boundary pressures are calculated on each node of the mesh using the equations,

$$P_{c_{i,j}}=\frac{16\sqrt{2}}{15}\pi(\sigma\eta\zeta)^2E\frac{\sqrt{\sigma}}{\sqrt{\zeta}}F\left(h_{i,j}/\sigma\right) \quad (8)$$

and

$$F(x) = \int (s-x)^{5/2} e^{(-s^2/2)} ds \tag{9}$$

where, parameters such as asperity density η, radius of curvature of asperity tops ζ, asperity heights σ, and composite elastic modulus E for the contacting material pairs, are the surface characteristics considered by the statistical model.

Wear is the progressive damage, involving material loss, which occurs on the surface of a component as a result of its motion relative to the adjacent working parts. It is the almost inevitable companion of the boundary friction. The wear rate of a rolling or sliding contact is usually defined as the volume of material lost from the wearing surface per unit sliding distance and is investigated with the Archard wear equation (Archard, 1953) [10];

$$\varpi = k \frac{W}{Hr} \tag{10}$$

where, ϖ is the wear rate in volume per distance, W is the wear load, Hr is the hardness of the sliding material, U is the sliding speed. The dimensionless constant k is known as the wear coefficient and its value is vital in application of equation (9). The constant k is difficult to obtain, but for a comparative study it is important to hold it constant during the all parametric work.

For the calculation of the wear rate the following equation is used in the code which gives wear of volume of material per second;

$$WearRate.\left[m^3/s\right] = k \frac{\frac{1}{T}\int_0^T \int_A P_c U dA.dt}{Hr.9.81x10^6} \tag{11}$$

where T is the period of 360° crank rotation. The contact pressure is calculated using the boundary contact model using equation (8).

Hydrodynamic power loss, which is related to viscous friction of the lubricant and boundary power loss due to boundary contact friction is calculated using the following equations. For hydrodynamic power loss;

$$\mathrm{IP}_{hyd} = \int_A \tau . U dA \tag{12}$$

where, for standard Reynolds' equation shear stress is found using:

$$\tau = \mu \frac{\partial U}{\partial y} = \mu \frac{U}{h} \tag{13}$$

For boundary power loss;

$$\mathrm{IP}_{bdy} = \int_A f . P_c . U . dA \tag{14}$$

where, f is the friction coefficient, U is the sliding velocity and P_c is the boundary contact pressure calculated using equation (8).

Piston dynamics parameters such as; piston axial velocity, piston axial acceleration, piston inertial behavior versus crank rotational speed, are solved by analyzing the slider crank mechanism.
The approach presented in [2] is used for the overall solution of the piston lubrication;

- First for a given cylinder pressure slider crank dynamics are solved and the side load on the piston is calculated.
- For a given side load Newton Raphson Method is used for the solution of equations of motion.
- In the Newton Rapshon iteration for each perturbation, for the estimated piston eccentricity and piston tilt with respect to cylinder axis, first the clearance between piston and cylinder is calculated.

- Knowing the film thickness around the piston, oil hydrodynamic pressure distribution is calculated by the solution of discreted form of Reynolds' equation.
- After integration of hydrodynamic and boundary contact pressures, the force balance in lateral direction and moment balance are solved.
- The iteration is continued until convergence. Then the solution is advanced to next time step.
- The entire solution is repeated until cyclic convergence is achieved.

3. RESULTS AND DISCUSSION

Real data of a compressor during an ongoing development project in Arçelik Compressor Plant is used for the parametric study. The results describing the piston dynamics are given as the film thicknesses of the piston thrust plane head and skirt sides and piston anti thrust plane head and skirt sides. The abbreviations skirt_t, skirt_at, head_t, head_at stand for skirt thrust side film thickness, skirt anti thrust side film thickness, head thrust side film thickness, head anti thrust side film thickness respectively. Also the calculated power loss values and wear rates are given comparatively.

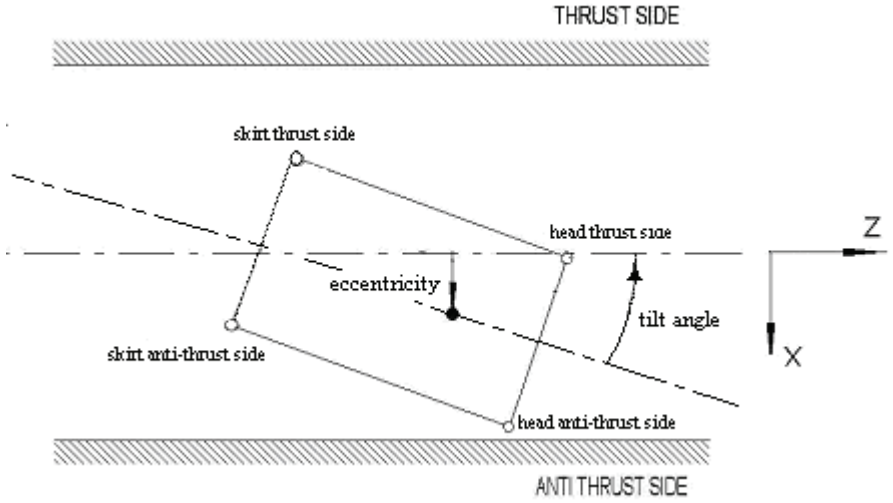

Figure 1 Piston locations of which film thicknesses are presented

5.3.4 Effect of Groove

The effect of groove is studied by changing groove location and groove width. First the effect of groove existence is investigated. A piston model without groove is named as no groove in Figure 2, Figure 3 and Figure 4 and compared with the base piston model with a groove that is 2.82 mm wide and located 7.04 mm away from skirt side. The piston studied has diameter of 25.40 mm and 16.57 mm length.

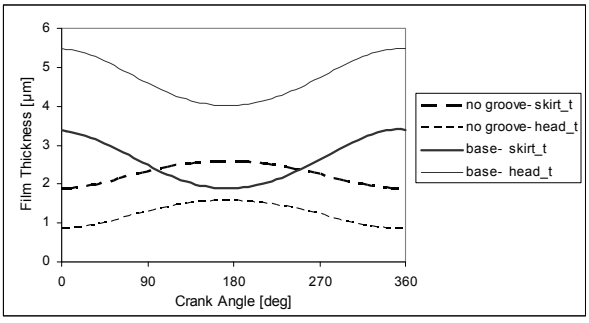

Figure 2 Piston thrust side skirt and head film thicknesses for pistons with groove and without groove

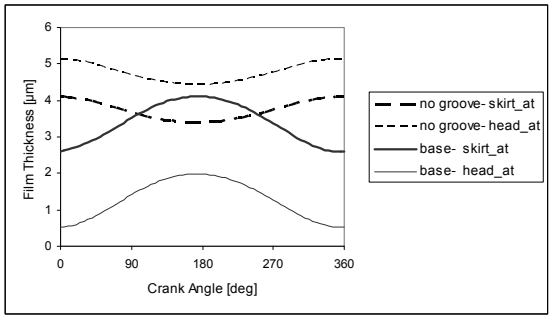

Figure 3 Piston anti thrust side skirt and head film thicknesses for pistons with groove and without groove

A commentary on Figure 2 and Figure 3 shows that the piston without groove works with negative tilt angle at thrust side. The tilt angle of piston without groove is smaller in magnitude than the base piston model with

groove, and also eccentricity variation is smaller. As the lubricated area of the piston without groove is larger, oil film pressure is lower, so smaller squeezing eccentric movements, and smaller tilt angle for the wedge effect are sufficient. As a result, minimum film thickness given in Figure 4 is thicker between crank angles about 280˚ – 80˚ for the piston without groove.

The primary motivation for using a groove is to reduce the sliding bearing area hence to reduce the power loss because of the reduction of hydrodynamic losses. On the other hand possible increase in the boundary power loss must stay in an acceptable range, which is the designer's decision. In Table 1 as expected there is 1 W decrease in hydrodynamic losses beside 0.03 W increase in boundary losses by the application of groove. There is slight increase in wear as a result of higher boundary forces. So from power loss point of view using a piston with groove is advantageous.

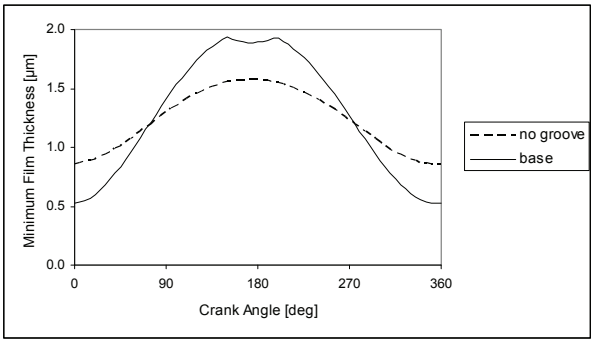

Figure 4 Minimum film thickness plots for pistons with groove and without groove

Table 1 Power loss and wear rates for pistons with and without groove

Case	*Power Loss [W]*		*Wear*
	Hydrodynamic	*Boundary*	
no groove	3.82	0.03	1.28E-14
base	2.87	0.06	4.05E-14

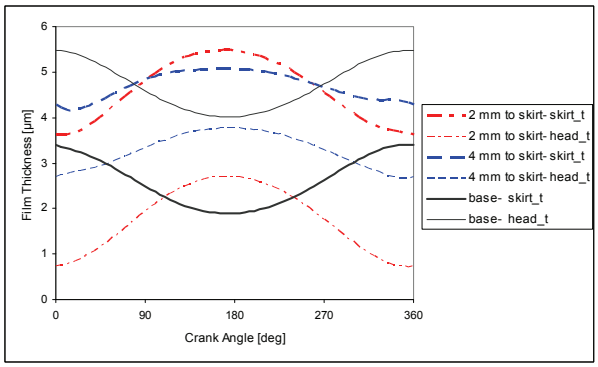

Figure 5 Piston thrust side skirt and head film thicknesses for pistons with grooves moved to skirt side

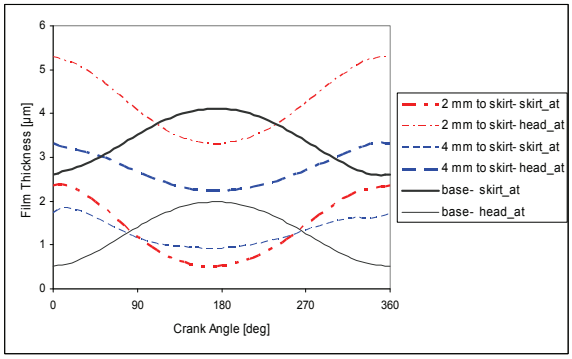

Figure 6 Piston anti thrust side skirt and head film thicknesses for pistons with grooves moved to skirt side

Moving the groove 4 mm decreases boundary power loss and wear rate since there is a significant increase in minimum film thickness for crank angles 270˚ -360˚. The minimum film thickness is lower than the base model between 90˚ - 270˚ but it is not lower than 1 µm. On the other hand, minimum film thickness of the base model is almost 0.5 µm at 0˚ (360˚) crank angle (Figure 7). So at overall cycle the film thickness does not fall below 1 µm for 4 mm groove location change.

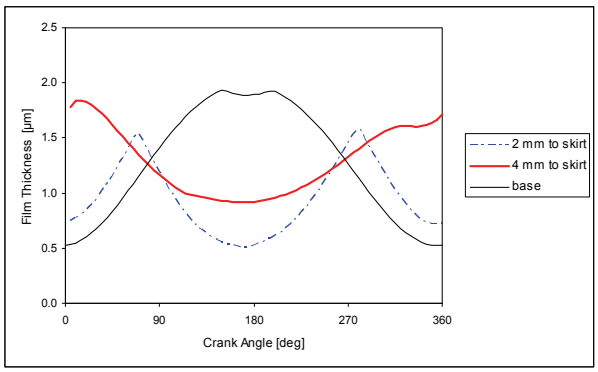

Figure 7 Minimum film thickness plot for pistons with grooves moved to skirt side

Table 2 Power loss and wear rates for pistons with grooves moved to skirt side

Case	*Power Loss [W]*		*Wear*
	Hydrodynamic	*Boundary*	
2 mm to skirt	2.91	0.19	1.49E-13
4 mm to skirt	2.88	0.01	6.05E-15
base	2.87	0.06	4.05E-14

The groove is moved to head side, and the results are compared with base piston model in Figure 8, Figure 9 and Figure 10. From the skirt thrust side and head anti thrust side plots it is clear that moving the groove to head side decreases the film thickness with respect to base piston, causing heavier working conditions. Similar conclusion can be reached form minimum film thickness plot in Figure 10 in which drastic decrease in minimum film thickness is observed.

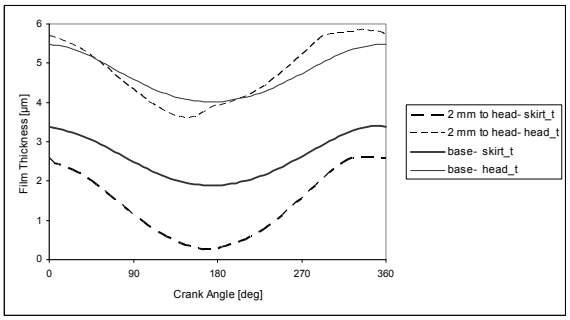

Figure 8 Piston thrust side skirt and head film thicknesses for piston with groove moved to head side

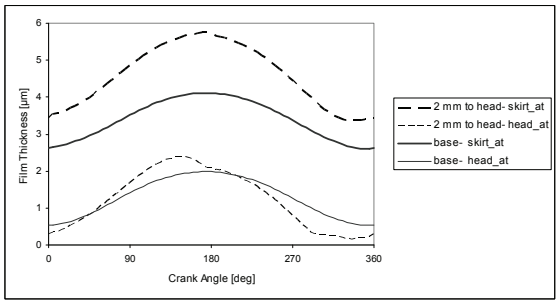

Figure 9 Piston anti thrust side skirt and head film thicknesses for piston with groove moved to head side

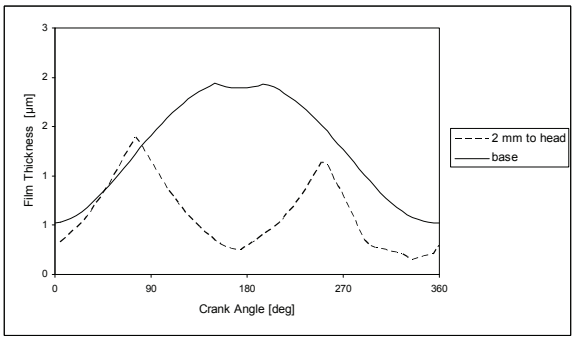

Figure 10 Minimum film thickness plot for pistons with grooves moved to skirt

Table 3 Power loss and wear rates for piston with grooves moved to head side

Case	*Power Loss [W]*		*Wear Rate*
	Hydrodynamic	*Boundary*	
2 mm to head	3.16	4.33	2.05E-12
base	2.87	0.06	4.05E-14

From the power loss and wear rate results in Table 3 the severe working conditions of the modified piston can be observed. The boundary power loss increases to a higher value than the hydrodynamic loss by a 4.27 W jump with respect to the base. And there is a significant increase in wear rate as result.

The results of groove location study verify that it is better to study the effect of groove width by extending it in skirt direction. The groove width is increased 2 mm and 4 mm to skirt side. Furthermore, the 2 mm wider groove is moved 2 mm to skirt side as an additional case. The results for skirt/head thrust/anti thrust sides' film thicknesses are given in Figure 11 and Figure 12. In the related graphics w2 stands for 2 mm wider, w4 stands for 4 mm wider groove, w2m2 stands for 2 mm wider groove that is also moved 2 mm to skirt side.

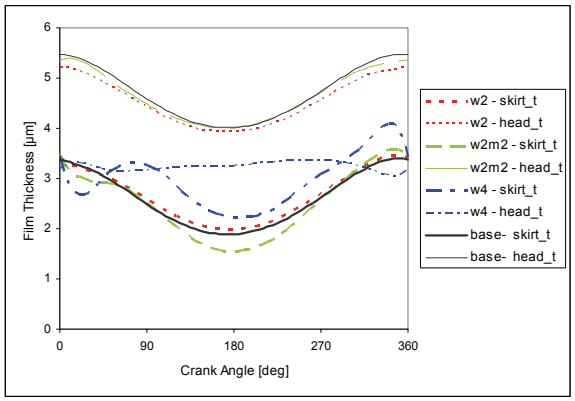

Figure 11 Piston thrust side skirt and head film thicknesses for piston with different groove widths

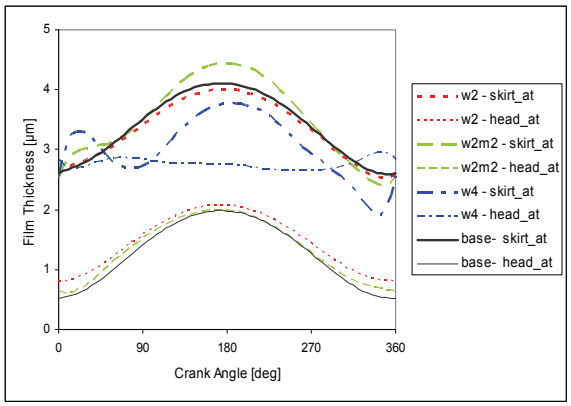

Figure 12 Piston anti thrust side skirt and head film thicknesses for piston with different groove widths

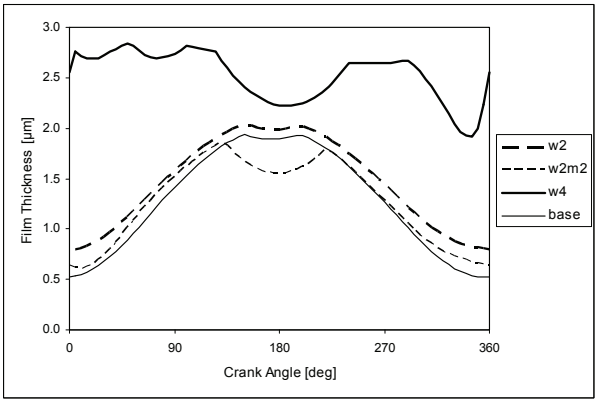

Figure 13 Minimum film thickness plots for pistons with different groove widths

Table 4 Power loss and wear rates for pistons with different groove widths

Case	*Power Loss [W]*		*Wear*
	Hydrodynamic	*Boundary*	
w2	2.46	0.02	1.14E-14
w2m2	2.53	0.10	6.00E-14
w4	1.83	0.00	0.00E+00
base	2.87	0.06	4.05E-14

For the cases that the groove is 2 mm wider (w2) and is 2 mm wider and moved 2 mm to skirt side (w2m2), the results of piston secondary dynamics are very similar to the base model. Because of the reduction in sliding bearing surface area, there is a decrease in hydrodynamic power loss (Table 4).

For the case of 4 mm wider groove, piston works almost at the center of the cylinder with a very small tilt angle. The film thickness around head side is almost uniform and close to 3 µm which can be observed from Figure 11, Figure 11 and minimum film thickness plot, Figure 12. For the skirt side there is a variation between 2 µm and 4 µm film thickness. So the piston does not work in boundary lubrication regime and has no boundary power loss as given in Table 4. And as a result of the wider groove, the hydrodynamic power loss decreases to 1.83 W from 2.87 W since increasing the groove width reduces the bearing area.

4. CONCLUSION

Hydrodynamic model for piston-cylinder bearing is developed and a parametric study is done related with the circumferential groove design. Under the restriction of rigid surfaces assumption and finite difference approach, it is observed that using a groove is advantageous from power loss point of view as the power loss decreases

with decreasing sliding bearing area. Without changing the width, moving the groove of the base model to head side should be avoided since it causes very low oil film formation and boundary lubrication. Moving and extending the groove to skirt side decreases power loss and wear rates. Finally, for the illustrated piston with a groove extended 4 mm to skirt side, complete hydrodynamic lubrication conditions are achieved.

In all applications the piston works with very small and almost constant tilt angle. This minimizes the load carrying capacity of the wedge effect. Hence it can be concluded that the load is primarily carried by the squeezing action of the piston that is formed by the eccentricity variation. Very small eccentric motions can cause serious hydrodynamic pressures since the piston of the case study works with very small radial clearance of 2.5 μm.

NOMENCLATURE

c	radial clearance	m
E	composite elastic modulus	Pa
e	piston eccentricity	m
f	friction coefficient	-
h	nominal film thickness	m
h_{dyn}	clearance due to geometry	m
h_{grv}	clearance due to groove	m
Hr	hardness	Pa
k	wear coefficient	-
L	bearing axial length	m
L_h	length from piston head to groove	m
l	connecting rod length	m
P	hydrodynamic oil pressure	Pa
P_c	boundary contact pressure	Pa
P_{gas}	cylinder gas pressure	Pa
P_{sc}	suction pressure	Pa
R	piston radius	m
t	time	s
T	compressor time period	s
U, U_z	sliding velocity of the piston	m/s
W	wear load	N
z	piston axial position	m
λ	piston tilt angle	rad
μ	viscosity of the lubricant	Pa.s
θ	angular coordinate on the piston	rad
η	asperity density	number/m^2
ζ	radius of curvature of asperity tops	m
σ	asperity heights	m
ϖ	wear rate	m^3/s
τ	shear stress	Pa
IP_{hyd}	hydrodynamic power loss	W
IP_{bdy}	boundary power loss	W

Subscripts

i	finite difference mesh index
j	finite difference mesh index

REFERENCES

[1] Goenka, P. K., and Meernik, P. R., 1992, Lubrication Analysis of Piston Skirts, SAE Paper 920490.
[2] Dursunkaya, Z., Keribar, K., 1992, "Simulation of Secondary Dynamics of Articulated and Conventional Piston Assemblies", SAE Paper No. 920484.
[3] Keribar, K., Dursunkaya, Z., 1992, "A Comprehensive Model of Piston Skirt Lubrication", SAE Paper No. 920483.
[4] Keribar, R., Dursunkaya, Z., and Ganapathy, V., 1993, "An Integrated Design Analysis Methodology to Adress Piston Tribological Issues", SAE Paper No. 930793.

[5] Duyar, M. and Dursunkaya, Z., "Design Improvement of a Compressor Bearing Using an Elastohydrodynamic Lubrication Model," International Compressor Engineering Conference at Purdue, July 16-19, West Lafayette Indiana, USA, 2002.
[6] Duyar, M. and Dursunkaya, Z., "Design Improvement Based on Wear of a Compressor Bearing Using an Elastohydrodynamic Lubrication Model," International Compressor Engineering Conference at Purdue, July 17-20, 2006 West Lafayette Indiana, USA.
[7] Sommerfeld, A., 1904, "Zur Hydrodynamichen Theorie der Schiermittelreibung", Z. angew. Math. Phys., 50, pp.97-155.
[8] McCool, J., I., 1988, "The Distrubution of Microcontact Area, Load, Pressure, and Flash Temperature Under the Greenwood-Williams Model", ASME Journal of Tribology, Vol.110, pp.106-111
[9] Greenwood, I. A., and Tripp, J. H., 1971, "*The Contact of Two Nominally Flat Surfaces"*, Proc. IMechE., Vol. 185, pp. 625-633.
[10] Archard, J., F., 1953, "Contact of Rubbing Flat Surfaces", Journal of Applied Physics, Vol. 24, pp.981-988